

## Identification of Hysteresis Loops

K.-H. HOFFMANN AND J. SPREKELS

*Institut für Mathematik, Universität Augsburg,  
Augsburg, West Germany*

AND

A. VISINTIN

*Universita Degli Studi di Trento, Trento, Italy*

Received November 3, 1986

A classical model representing several hysteresis phenomena (as they appear in ferromagnetism and in porous media filtration, e.g.) is considered here. It is demonstrated that the parameters of this model can be determined with any desired precision from suitable experiments. We use the mathematical model of hysteresis as introduced by Preisach, who explained the magnetization curve and saturation loop of the material by a superposition of elementary rectangular loops. A certain properly defined measure is responsible for the shape of the loop. We describe a new algorithm which determines this measure completely. Our results are related to previous papers of Biorci and Pescetti. Extensive numerical computations conclude our investigations. © 1988 Academic Press, Inc.

### 1. INTRODUCTION

In this note we deal with an algorithm for the identification of nonlinearities of hysteresis type in rather general deterministic systems. The mathematical model to be chosen is crucial in our approach. It has turned out that Preisach's idea of describing hysteresis is also very convenient for our purpose. From input-output measurements we are able to compute completely the distribution of the thresholds of the elementary rectangular loops in the "Preisach plane." Hysteresis phenomena appear in several fields: in ferromagnetism (studied in Preisach's paper, e.g.), in filtration through porous media, in elasto-plasticity, in biology, etc. However, until now only comparably few mathematical papers have been published in this field. The state of the art up to 1983 is summarized in a recently published book of Krasnoselskii and Pokrovskii [1] which will also appear in English translation soon. As far as the inverse problem of identifying hysteresis loops from measurements is concerned, we do not know of more than a dozen more or less mathematically oriented published contributions. Our work is related to previously published papers of Biorci and Pescetti [4-6], who give an analytical theory of

ferromagnetism using Preisach's approach. They are able to develop an algorithm for determining the "Preisach measure" at any point in the "Preisach plane" arbitrarily accurately. Our method, on the other hand, determines the whole measure by an approximation technique which is based on a finite number of optimally chosen input-output experiments. One should also mention the paper of Andronikou, Bekey, Hadaegh [2] which deals with the identifiability of a damped harmonic oscillator containing hysteretic restoring forces. Their results are concerned with structural identifiability conditions in the sense of Bellman and Astrom [3]. Although their hysteresis model differs from ours, our algorithm applies to their example as well. But the aspect of structural identifiability is not the object of our present investigations.

Our paper is organized as follows: In Section 2 we introduce the Preisach model of hysteresis and indicate some important properties. Here we just report the main mathematical results, referring to Visintin [8, 10] for details. Section 3 contains the approximation scheme for the measure and formulates the special identification procedure we want to present. Finally, Section 4 has some numerical experiments demonstrating the practicability of our algorithm. Some concluding remarks give hints for further applications of our identification method.

## 2. THE PREISACH MODEL

Let  $\rho = (\rho_1, \rho_2)$ ,  $\rho_1 < \rho_2$ , be a couple of thresholds of an elementary rectangular hysteresis loop in the  $(\rho_1, \rho_2)$ -plane. We introduce the "Preisach plane"  $\mathcal{P}$ ,

$$\mathcal{P} := \{\rho = (\rho_1, \rho_2) \in \mathbb{R}^2 \mid \rho_1 < \rho_2\},$$

and we define the "relay operator"  $f_\rho$  for each  $\rho \in \mathcal{P}$ .

Let  $T > 0$  and  $s \in C^0[0, T]$ . For any  $\xi \in \{0, 1\}$ , the measurable mapping

$$f_\rho(s, \xi): [0, T] \rightarrow \{0, 1\}$$

is defined by

$$[f_\rho(s, \xi)](0) := \begin{cases} 0 & \text{if } s(0) \leq \rho_1, \\ \xi & \text{if } \rho_1 < s_0 < \rho_2, \\ 1 & \text{if } s(0) \geq \rho_2, \end{cases} \quad (2.1)$$

and for  $t \in (0, T]$ , setting  $A_t := \{\tau \in (0, t] \mid s(\tau) = \rho_1 \text{ or } s(\tau) = \rho_2\}$ , by

$$[f_\rho(s, \xi)](t) := \begin{cases} [f_\rho(s, \xi)](0) & \text{if } A_t = \emptyset, \\ 0 & \text{if } A_t \neq \emptyset \text{ and } s(\max A_t) = \rho_1, \\ 1 & \text{if } A_t \neq \emptyset \text{ and } s(\max A_t) = \rho_2. \end{cases} \quad (2.2)$$

For any  $\rho \in \mathcal{P}$ , this construction defines a (discontinuous) operator  $f_\rho: C^0[0, T] \times \{0, 1\} \rightarrow L^\infty(0, T)$ . This may represent the behaviour of a relay with hysteresis:

- $\rho_1$  and  $\rho_2$  are the thresholds,
- $s$  and  $f_\rho(s, \xi)$  are the “input” (or “control”) and “output” (or “state”) variables, respectively,
- $\xi$  is the initial state of the relay.

More general hysteresis representations are obtained by considering averages of “relay operators”  $f_\rho$  with different thresholds  $\rho$ , according to a prescribed “relay density.”

We fix a  $\sigma$ -algebra  $\mathcal{A}$  of measurable subsets of  $\mathcal{P}$  and consider a family  $\mathcal{S}$  of  $\mathcal{A}$ -measurable applications from  $\mathcal{P}$  into  $\{0, 1\}$ . Let  $\mu$  be a positive finite measure on  $\mathcal{A}$ . With respect to  $\mu$ , the “Preisach hysteresis functional”  $M_\mu$  is defined as follows:

For any “input function”  $s \in C^0[0, T]$ , any “initial configuration”  $w^0 \in \mathcal{S}$  and any  $t \in [0, T]$ , we set

$$[M_\mu(s, w^0)](t) := \int_{\mathcal{P}} [f_\rho(s, w_\rho^0)](t) d\mu_\rho \quad (2.3)$$

(here  $w_\rho^0$  represents the initial state of the relay characterized by the threshold  $\rho = (\rho_1, \rho_2)$ ). This construction defines the (in general discontinuous) “Preisach hysteresis operator”  $M_\mu: C^0[0, T] \times \mathcal{S} \rightarrow L^\infty(0, T)$ . However, the following properties were proved by Visintin in [8]:

PROPOSITION 1. *If*

$$\mu \text{ has no masses concentrated either in points or along segments parallel to the axes,} \quad (2.4)$$

then

$$M_\mu(s, w^0) \in C^0[0, T], \quad \text{for all } s \in C^0[0, T] \text{ and all } w^0 \in \mathcal{S}, \quad (2.5)$$

$$\text{the operator } s \mapsto M_\mu(s, w^0) \text{ is continuous in } C^0[0, T] \text{ with respect to the uniform convergence.} \quad (2.6)$$

A similar, but weaker, result was proved by Friedman and Hoffmann [9]. Henceforth we shall fix the initial state  $w^0$  by setting

$$w_\rho^0 := \begin{cases} 1 & \text{if } \rho_1 + \rho_2 \leq 0, \\ 0 & \text{if } \rho_1 + \rho_2 > 0. \end{cases} \quad (2.7)$$

This means, we assume that the material is initially in the virginal state. In the case of ferromagnetism, this means that the material has not yet experienced any magnetization (Fig. 1).

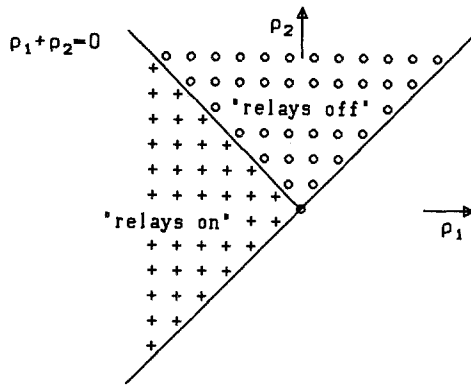


FIG. 1. Initial state of the relays.

Then the argument  $w^0$  will be substituted into the relay operator  $f_\rho$  and, correspondingly, into the hysteresis functional  $M_\mu$ . However, all the results we get can be extended to the case of a general  $w^0 \in \mathcal{S}$ .

One of the main advantages offered by the Preisach model is its geometrical interpretation. This allows a better understanding of its properties and can be useful for computations. We sketch the main features here, referring to Visintin [8, 10] for details.

For any fixed  $s \in C^0[0, T]$  and any  $t \in [0, T]$ , we set

$$p_\rho := [f_\rho(s, w_\rho^0)](t) \tag{2.8}$$

for all  $\rho \in \mathcal{P}$ . Then  $p \in \mathcal{S}$ , and  $\mathcal{P}$  defines a partition  $\{\mathcal{P}_p^+, \mathcal{P}_p^0\}$  of  $\mathcal{P}$ :

$$\begin{aligned} \mathcal{P}_p^+ &:= \{\rho \in \mathcal{P} \mid p_\rho = 1\}, \\ \mathcal{P}_p^0 &:= \{\rho \in \mathcal{P} \mid p_\rho = 0\}. \end{aligned} \tag{2.9}$$

It is easy to verify that

$$\begin{aligned} \{\rho \in \mathcal{P} \mid \rho_1 > \tilde{\rho}_1, \rho_2 > \tilde{\rho}_2\} &\subset \mathcal{P}_p^0, & \text{for all } \tilde{\rho} \in \mathcal{P}_p^0, \\ \{\rho \in \mathcal{P} \mid \rho_1 < \tilde{\rho}_1, \rho_2 < \tilde{\rho}_2\} &\subset \mathcal{P}_p^+, & \text{for all } \tilde{\rho} \in \mathcal{P}_p^+. \end{aligned} \tag{2.10}$$

Hence the common boundary  $\mathcal{G} := \partial\mathcal{P}_p^+ \cap \partial\mathcal{P}_p^0$  is an antimonotone graph in the Preisach plane  $\mathcal{P}$  as indicated in Fig. 2. More precisely, we have

**PROPOSITION 2** (Visintin [10]). *Let us assume that the initial configuration is defined as in (2.7). Then, for any  $s \in C^0[0, T]$  and any  $t \in [0, T]$ ,  $\mathcal{G}$ , defined as above, is a maximal antimonotone graph; it is composed of the half-line  $\{\rho \in \mathbb{R}^2 \mid \rho_1 + \rho_2 = 0, \rho_2 \geq \max_{\tau \in [0, t]} |s(\tau)|\}$  and of an at most countable family of segments parallel to the axes which may accumulate just in a neighbourhood of the point  $(s(t), s(t)) \in \mathcal{G}$ .*

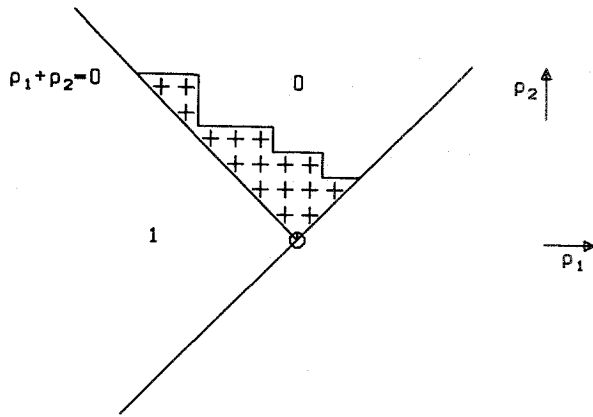


FIG. 2. Maximal antimonotone graph  $\mathcal{G} = \partial\mathcal{P}_p^+ \cap \partial\mathcal{P}_p^0$  (at any time instant  $t$ ,  $\mathcal{G}(t)$  describes the internal state of the system).

Due to these properties, it is easy to represent the evolution of  $\mathcal{G}(t)$  for any piecewise monotone continuous input functions  $s$ . These functions, however, form a dense subset of  $C^0[0, T]$ .

### 3. IDENTIFICATION OF THE MEASURE $\mu$

#### 3.1. Approximation of the Measure

Let  $\mu$  be absolutely continuous with respect to the two-dimensional Lebesgue measure  $\lambda$ . From the Radon–Nikodym theorem it follows that a positive function  $\varphi \in L^1(\mathcal{P})$  exists such that  $\mu(A) = \int_A \varphi(x) d\mu$ , for all measurable sets  $A \in \mathcal{A}$ . Obviously, this property is a sufficient (but not necessary) condition for (2.4); hence it entails (2.5) and (2.6), by Proposition 1.

Let us assume that the support  $\Sigma$  of  $\mu$  is bounded, and let  $\{\mathcal{R}_m\}_{m \in \mathbb{N}}$  be a family of partitions of  $\Sigma$  by rectangles with the property that

$$\delta_m := \max\{\text{diam } B \mid B \in \mathcal{R}_m\} \rightarrow 0, \quad \text{as } m \rightarrow \infty.$$

For any  $m \in \mathbb{N}$  and for almost any  $\rho \in \Sigma$ , we denote by  $B_\rho$  the element of  $\mathcal{R}_m$  such that  $\rho \in B_\rho$ , and we set

$$\varphi_m(\rho) := \begin{cases} \frac{\mu(B_\rho)}{\lambda(B_\rho)} & \text{if } \rho \in \Sigma, \\ 0 & \text{if } \rho \in \mathcal{P} \setminus \Sigma. \end{cases} \quad (3.1)$$

Clearly,  $\varphi_m \rightarrow \varphi$ , strongly in  $L^1(\mathcal{P})$ , as  $m \rightarrow \infty$ . Hence, setting  $d\mu_m := \varphi_m \cdot d\lambda$ , for any  $s \in C^0[0, T]$  and for any  $w^0 \in \mathcal{S}$  we have, by (2.3),

$$M_{\mu_m}(s, w^0) \rightarrow M_\mu(s, w^0), \quad \text{as } m \rightarrow \infty, \tag{3.2}$$

uniformly in  $[0, T]$  and uniformly with respect to  $s \in C^0[0, T]$ .

Thus the convergence properties of this approximation are quite satisfactory. In order to implement it, we have to evaluate  $\mu(B)$  for any  $B \in \mathcal{R}_m$ . This will require several tests, each consisting in applying a (finite) sequence of “inputs” and measuring the corresponding “outputs.”

In the case of ferromagnetism, one can take a toroidal sample of the material under consideration and wire a conducting coil around it. The input here corresponds to the intensity of the magnetic field  $H$ , which is proportional to the intensity of the electric current circulating in the wire. The output is the magnetization field  $M$  which (more precisely, the magnetic induction  $B := \mu_0 H + r\pi M$ ) can be measured by a standard procedure.

There are two basic strategies for conducting these tests:

(i)  $\mu(B)$  can be evaluated *separately* for each  $B \in \mathcal{R}_m$  by means of a simple test, as in Biorci and Pescetti [4–6].

(ii)  $\mu(B)$  can be evaluated *simultaneously* for all  $B \in \mathcal{R}_m$  by means of a more complex test.

The second strategy allows to reduce the overall number of measurements.

We notice that the procedure described above can be used also in the more general case where (2.4) holds, but  $\mu$  is not necessarily absolutely continuous with respect to the Lebesgue measure  $\lambda$ ; however, it is not obvious then that the convergence property (3.2) is still satisfied.

### 3.2. The Evaluation Procedure

As a particularly convenient partition  $\mathcal{R}_m$  of  $\Sigma$ , let us consider a mesh parallel to the axes; we also assume that the width of this mesh is uniform and equal to  $h := (|\Sigma L| + |\Sigma R|)/2m$ , for the sake of simplicity. Then we have to compute  $\mu_m(B)$ , for any  $B \in \mathcal{R}_m$ . We may assume that  $\Sigma$  is contained in a rectangle. As “input functions” a finite family of polygons  $s_m^n$  ( $n = 1, 2, \dots, 4m$ ) on  $\mathbb{R}_+$  is defined by

$$\begin{aligned} s_m^n(0) &:= \frac{|\Sigma L| + |\Sigma R|}{2}, & n = 1, 2, \dots, 4m, \\ s_m^n(2k - 1) &:= \frac{|\Sigma L| + |\Sigma R|}{2} - (k - 1) \frac{|\Sigma L| + |\Sigma R|}{2m}, & 1 \leq k \leq \left\lfloor \frac{n + 1}{2} \right\rfloor, n = 1, 2, \dots, 2m, \\ s_m^n(2k) &:= \frac{|\Sigma L| + |\Sigma R|}{2} - (n - k) \frac{|\Sigma L| + |\Sigma R|}{2m}, & 1 \leq k \leq \left\lfloor \frac{n}{2} \right\rfloor, n = 2, 3, \dots, 2m, \end{aligned} \tag{3.3}$$

linear in the subinterval  $[2k - 1, 2k]$  and constant outside. To complete this family of polygons we introduce

$$s_m^{2m+j}(t) := -s_m^{2m-j+1}(t), \quad j = 1, \dots, 2m. \quad (3.4)$$

Some elements of this family, as well as their corresponding traces in the Preisach plane  $\mathcal{P}$  are depicted in Fig. 3.

Let the measurements corresponding to the "input function"  $s_m^n$  at time instant  $t = \tau$  be denoted by  $v_n(\tau)$  and  $[v_n]_{\tau_2}^{\tau_1} := v_n(\tau_1) - v_n(\tau_2)$ . The squares in the partition  $\mathcal{R}_m$  will be labeled from right to left and from top to bottom, using double indices as indicated in Fig. 3. Accordingly, the approximation for the value of the function  $\varphi$  on the square  $B_{ij}$  is denoted by  $\varphi_{ij}$ .

Next we illustrate the algorithm which computes all the values  $\varphi_{ij}$  for the example  $m = 4$  (Fig. 3).

$$\begin{aligned} [v_2]_3^3 &= \varphi_{11} \\ [v_3]_3^3 &= \varphi_{11} + \varphi_{12} \\ [v_4]_3^3 &= \varphi_{11} + \varphi_{12} + \varphi_{13} & [v_4]_5^3 &= \varphi_{22} \\ [v_5]_3^3 &= \varphi_{11} + \varphi_{12} + \varphi_{13} + \varphi_{14} & [v_5]_5^3 &= \varphi_{22} + \varphi_{23} \\ [v_6]_3^3 &= \varphi_{11} + \varphi_{12} + \varphi_{13} + \varphi_{14} + \varphi_{15} & [v_6]_5^3 &= \varphi_{22} + \varphi_{23} + \varphi_{24} \\ [v_7]_3^3 &= \varphi_{11} + \varphi_{12} + \varphi_{13} + \varphi_{14} + \varphi_{15} + \varphi_{16} & [v_7]_5^3 &= \varphi_{22} + \varphi_{23} + \varphi_{24} + \varphi_{25} \\ [v_8]_3^3 &= \varphi_{11} + \varphi_{12} + \varphi_{13} + \varphi_{14} + \varphi_{15} + \varphi_{16} + \varphi_{17} & [v_8]_5^3 &= \varphi_{22} + \varphi_{23} + \varphi_{24} + \varphi_{25} + \varphi_{26} \\ \\ [v_6]_7^5 &= \varphi_{33} \\ [v_7]_7^5 &= \varphi_{33} + \varphi_{34} \\ [v_8]_7^5 &= \varphi_{33} + \varphi_{34} + \varphi_{35} & [v_8]_9^7 &= \varphi_{44} \\ \\ v_8(3) - v_9(2) &= \varphi_{18} \\ v_8(5) - v_9(4) &= \varphi_{18} + \varphi_{27} \\ v_8(7) - v_9(6) &= \varphi_{18} + \varphi_{27} + \varphi_{36} \\ v_8(9) - v_9(8) &= \varphi_{18} + \varphi_{27} + \varphi_{36} + \varphi_{45} \\ \\ [v_9]_1^3 &= \varphi_{28} + \varphi_{38} + \varphi_{48} + \varphi_{58} + \varphi_{68} + \varphi_{78} + \varphi_{88} & [v_9]_3^5 &= \varphi_{37} + \varphi_{47} + \varphi_{57} + \varphi_{67} + \varphi_{77} \\ [v_{10}]_1^3 &= \varphi_{38} + \varphi_{48} + \varphi_{58} + \varphi_{68} + \varphi_{78} + \varphi_{88} & [v_{10}]_3^5 &= \varphi_{47} + \varphi_{57} + \varphi_{67} + \varphi_{77} \\ [v_{11}]_1^3 &= \varphi_{48} + \varphi_{58} + \varphi_{68} + \varphi_{78} + \varphi_{88} & [v_{11}]_3^5 &= \varphi_{57} + \varphi_{67} + \varphi_{77} \\ [v_{12}]_1^3 &= \varphi_{58} + \varphi_{68} + \varphi_{78} + \varphi_{88} & [v_{12}]_3^5 &= \varphi_{67} + \varphi_{77} \\ [v_{13}]_1^3 &= \varphi_{68} + \varphi_{78} + \varphi_{88} & [v_{13}]_3^5 &= \varphi_{77} \\ [v_{14}]_1^3 &= \varphi_{78} + \varphi_{88} \\ [v_{15}]_1^3 &= \varphi_{88} \\ \\ [v_9]_5^7 &= \varphi_{46} + \varphi_{56} + \varphi_{66} & [v_9]_7^9 &= \varphi_{55} \\ [v_{10}]_5^7 &= \varphi_{56} + \varphi_{66} \\ [v_{11}]_5^7 &= \varphi_{66} \end{aligned}$$

These equations can be solved successively for  $\varphi_{ij}$ , where one should remark that the nine blocks of equations can be solved independently of each other. Therefore the algorithm can be very well adapted to parallel computing.

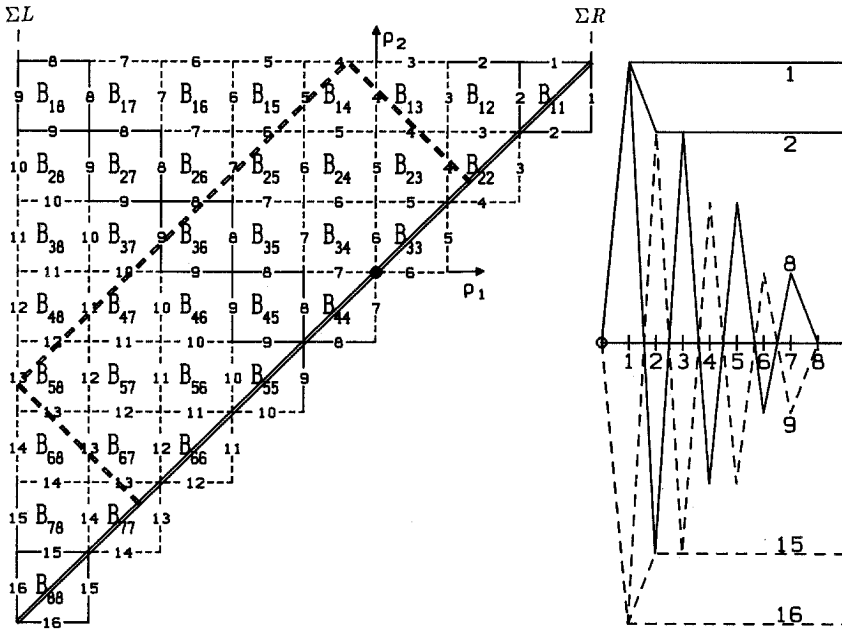


FIG. 3. "Input functions"  $s_4^1, s_4^2, s_4^8, s_4^9, s_4^{15}, s_4^{16}$  and corresponding traces  $\mathcal{G}(t)$  in the Preisach plane. Labels of the squares in the discretization.

In the general situation for arbitrary  $m$  one has to evaluate the following formulas:

$$\varphi_{jj} = [v_{2j}]_{2j+1}^{2j-1}; \quad j = 1, 2, \dots, m \tag{3.5}$$

$$\varphi_{kj} = [v_{j+k} - v_{j+k-1}]_{2k+1}^{2k-1}; \quad j = (k+1), \dots, 2m-k, k = 1, 2, \dots, m-1$$

$$\varphi_{jj} = [v_{2j-1}]_{2j-1}^{2j+1}; \quad j = m+1, \dots, 2m$$

$$\varphi_{j,2m-k+1} = [v_{j+2m-k} - v_{j+2m-k+1}]_{2k-1}^{2k+1}; \quad j = k+1, \dots, 2m-k, k = 1, 2, \dots, m-1 \tag{3.6}$$

$$\varphi_{1,2m} = v_{2m}(3) - v_{2m+1}(2) \tag{3.7}$$

$$\varphi_{j,2m-j} = [v_{2m}]_{2j+1}^{2j+2} - [v_{2m+1}]_{2j}^{2j+2}; \quad j = 1, 2, \dots, m-1$$

The total number of squares where  $\varphi$  has to be calculated is  $m(2m+1)$ , and the total number of turning points of the function  $s_m^n$  which are necessary in our procedure is  $2m(2m+1) - 2$ . If the efficiency of the algorithm is defined as the ratio between the number of squares to be evaluated and the number of necessary elementary operations (= the total number of the turning points of the inputs), our procedure has an efficiency which is asymptotically equal to 2. This means that we



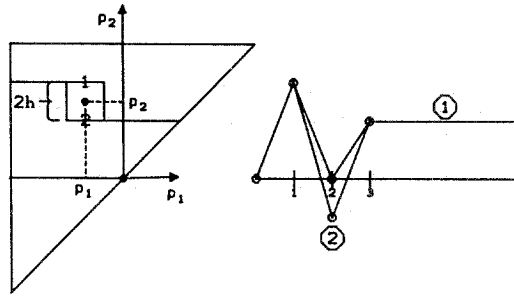


FIG. 4. "Input functions" and their corresponding  $\mathcal{G}(t)$  in the Preisach plane for the Biorci-Pescetti method.

asymptotically need one input function to calculate  $\varphi$  on a single square. Thus we have the statement:

**PROPOSITION 3.** *The algorithm (3.5), (3.6), (3.7) is optimal in the sense of the minimal number of elementary operations which are necessary to calculate  $\varphi$ .*

In contrast to our algorithm which simultaneously computes all of  $\varphi$ , Biorci and Pescetti proposed in their papers a method to calculate  $\varphi$  at one single point  $\rho = (\rho_1, \rho_2) \in \mathcal{P}$ . To explain their method, let us assume that the virginal state of the system is again defined by (2.4). Then choose a steplength  $h > 0$  and substitute the two "input functions"  $s_h^1, s_h^2$  into the system, measuring the corresponding "output values"  $v_h^1(i), v_h^2(i)$  ( $i = 1, 2, 3$ ). The polygons  $s_h^j$  ( $j = 1, 2$ ) are defined by their vertices:

$$\begin{aligned} s_h^1(0) &= 0, & s_h^1(1) &= \rho_2 + h, & s_h^1(2) &= \rho_1 + h, & s_h^1(3) &= \rho_2 - h, \\ s_h^2(0) &= 0, & s_h^2(1) &= \rho_2 + h, & s_h^2(2) &= \rho_1 - h, & s_h^2(3) &= \rho_2 - h. \end{aligned}$$

The function value  $\varphi(\rho)$  is obtained by the difference

$$v_h^1(3) - v_h^2(3).$$

Clearly this algorithm has the complexity 4 according to our definition of efficiency. This means that two "input functions" are necessary to measure one square (compare Fig. 4).

#### 4. NUMERICAL EXPERIMENTS

We have tested our method in a series of numerical experiments, and we present a small selection of the results. The accuracy of the approximations was very satisfactory; the only significant deviations from the true measure were observed in a small neighbourhood (corresponding to the mesh-width of the grid) of the boun-

dary of the support of  $\varphi$ . This is caused by the fact that only parts of the boundary squares of the discretization are contained in the support of  $\varphi$ . Therefore the (constant) value of  $\varphi$  on these squares is also smeared over those parts of the squares where the true  $\varphi$  is equal to zero. With refinements of the grid these errors decrease.

Our experiments are performed as follows: First we simulate measurements  $v_n(\tau)$  by prescribing a measure  $\mu$  (resp. a function  $\varphi$ ) and substituting the “input functions” (3.3), (3.4) into formula (2.3). After that, we forget  $\varphi$  and recover it

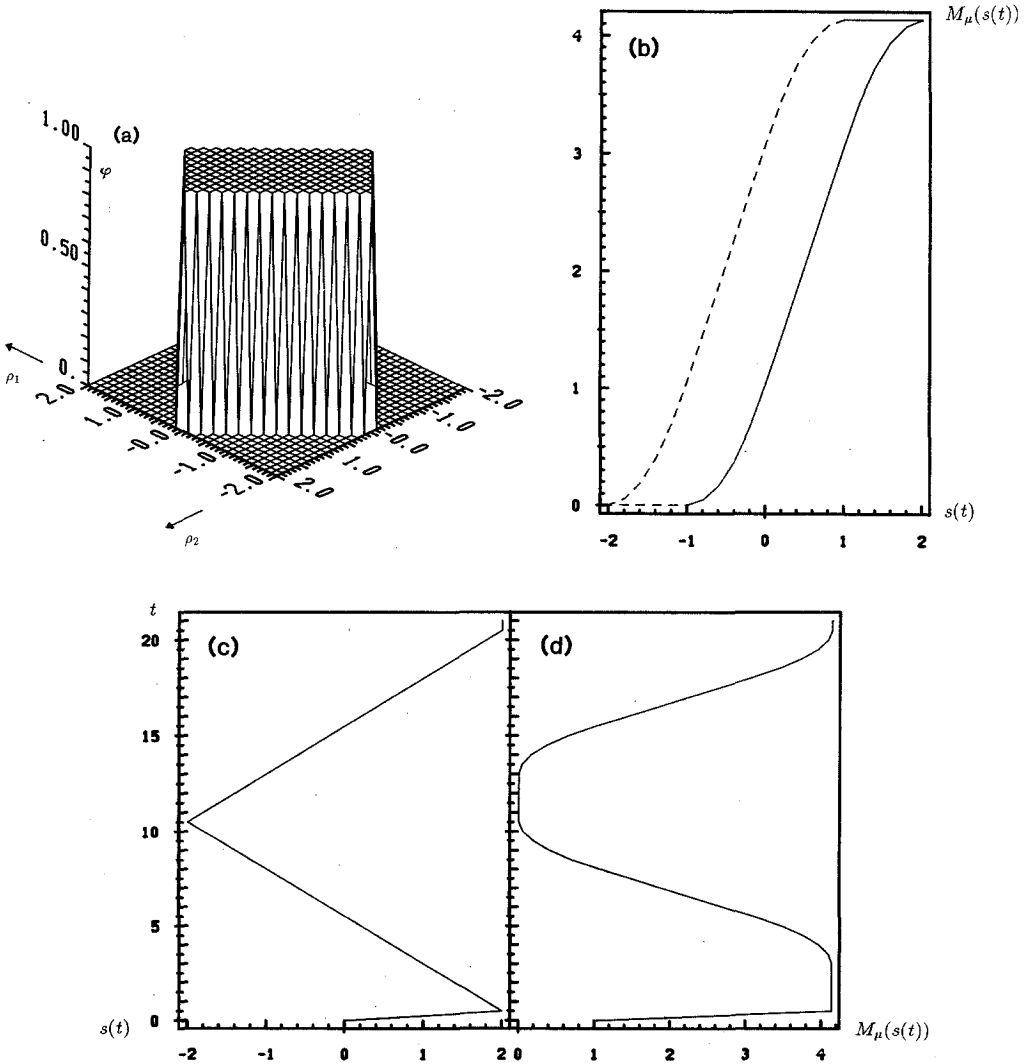


FIG. 5. Example 1.

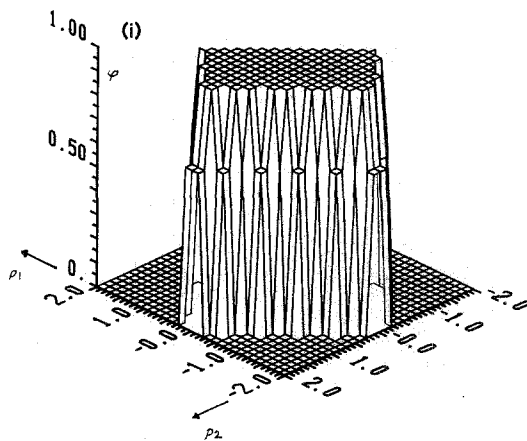
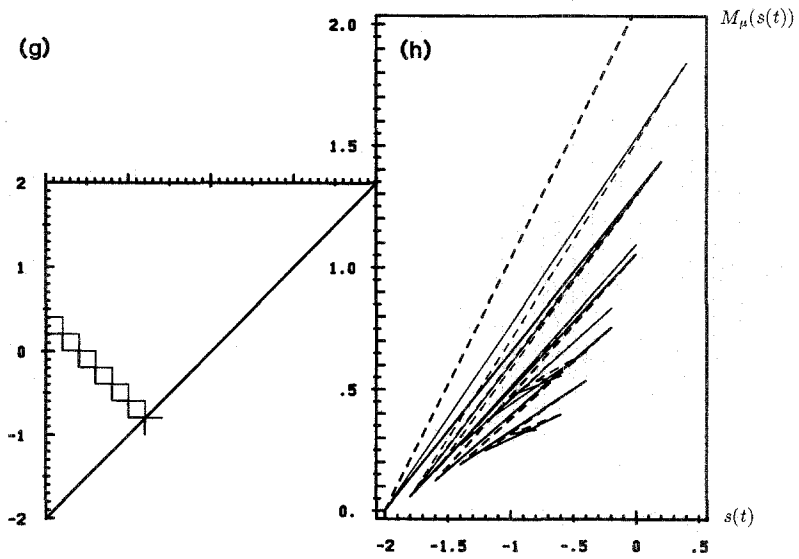
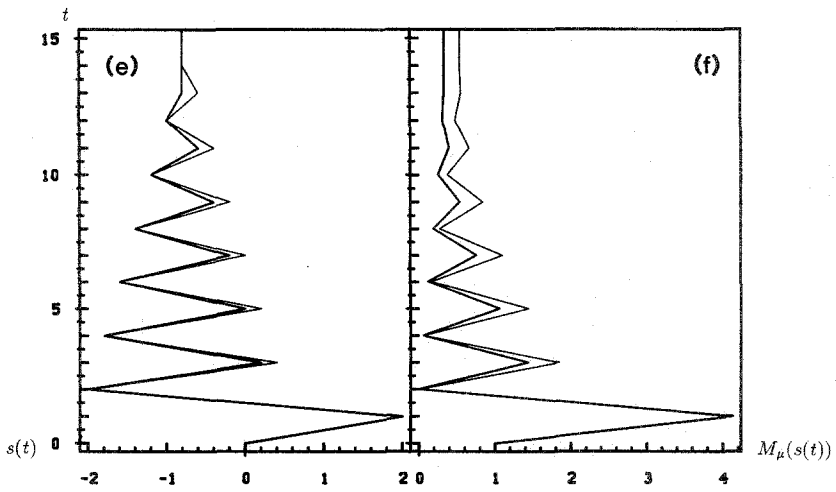


FIG. 5—Continued.

approximatively by evaluating formulas (3.5), (3.6), (3.7) according to our algorithm. The plots at the end of this paper show our results. Therefore the meaning of the letters (a), (b), ... in the figures for Examples 1-3 is:

- (a) the true function  $\varphi$ ,
- (b) the hysteresis loop corresponding to  $\varphi$ ,
- (c) the "input function," which produces this loop,
- (d) the "output function" corresponding to this loop,

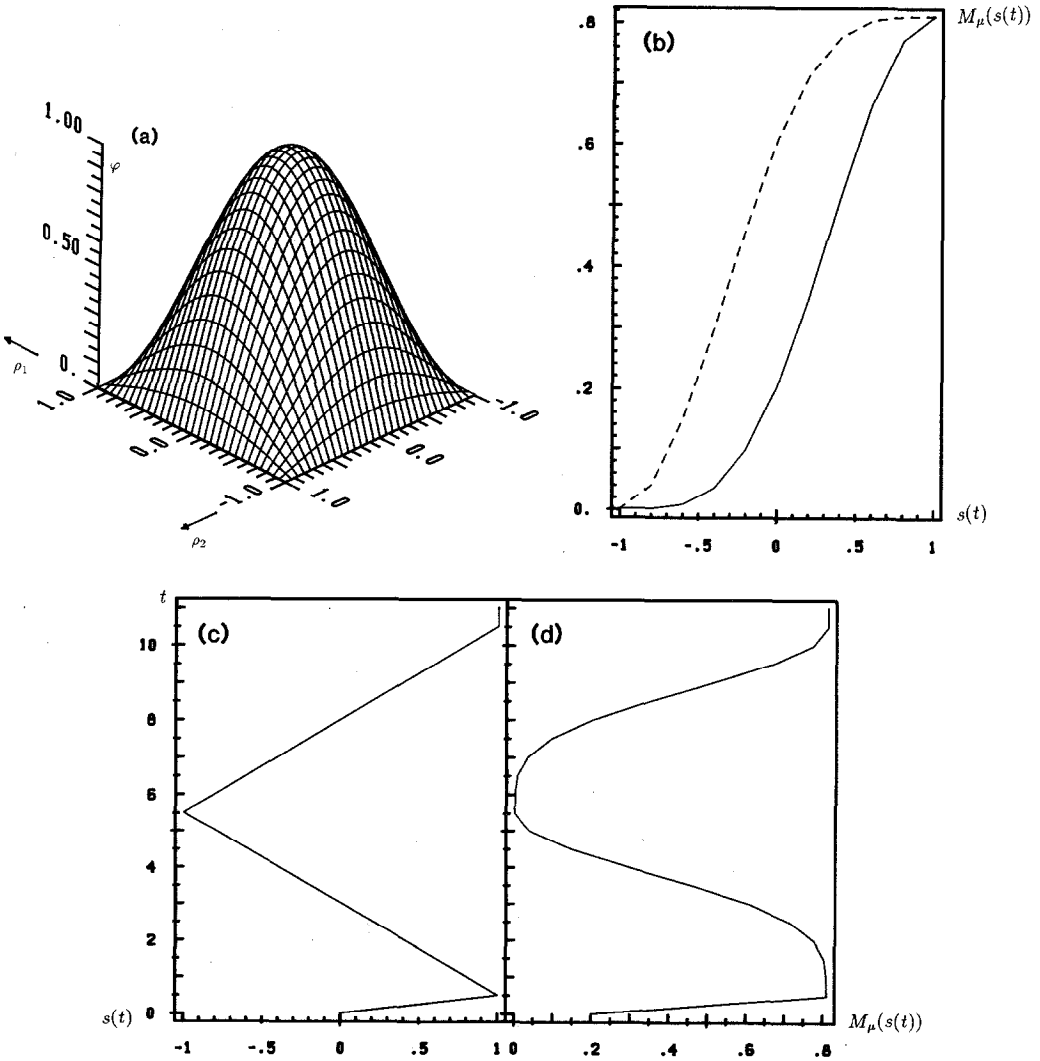


FIG. 6. Example 2.

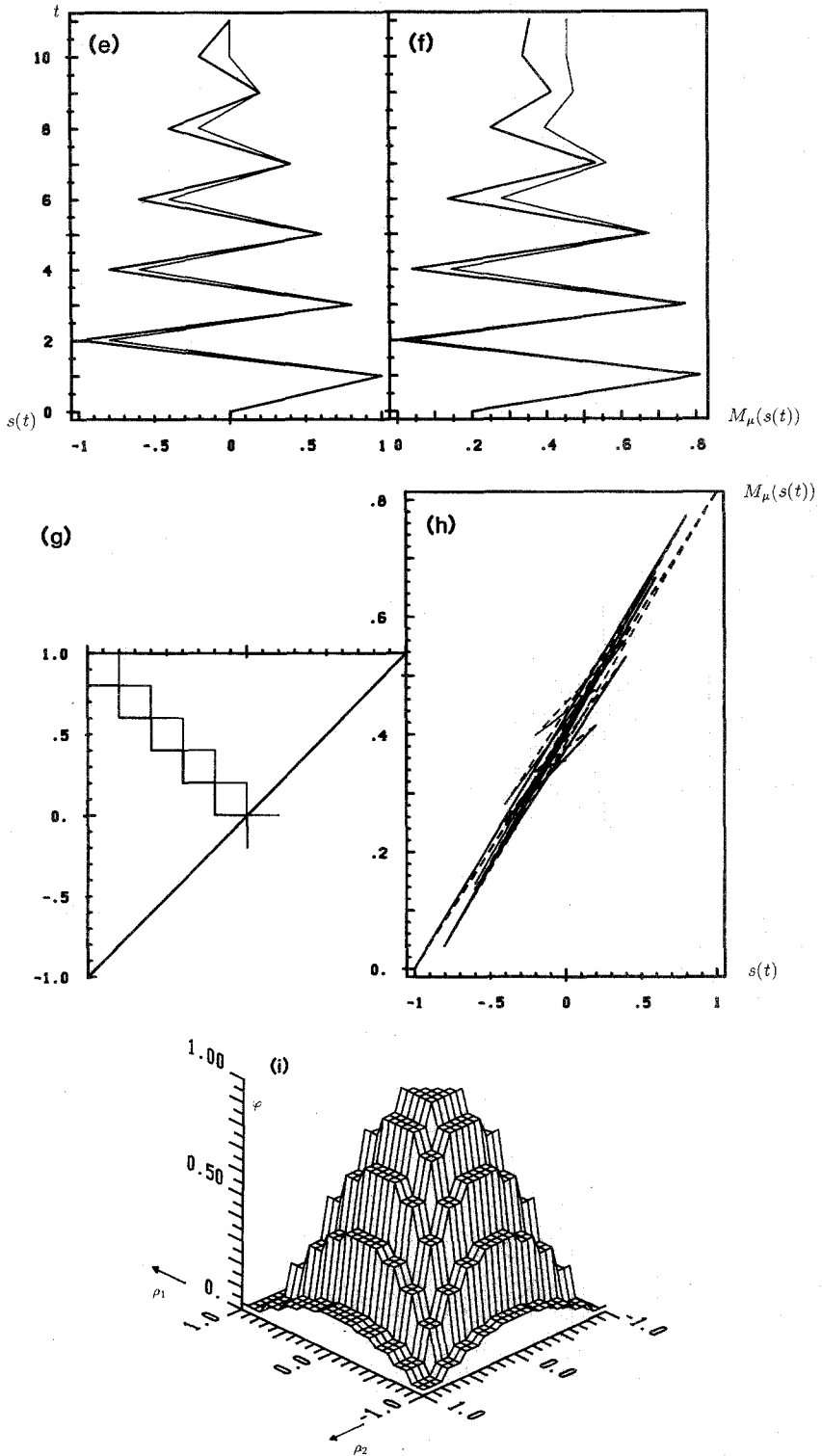


FIG. 6—Continued.

- (e) the test "input functions"  $s_m^n(t)$ ,
- (f) the values of the corresponding "output function,"
- (g) the trace  $\mathcal{G}(t)$  in the Preisach plane  $\mathcal{P}$ ,
- (h) the corresponding path within the hysteresis loop,
- (i) the identified function  $\varphi$ .

EXAMPLE 1.  $\Sigma L = -2, \Sigma R = 2, m = 20: \varphi(\rho_1, \rho_2) \equiv 1$  for  $\rho \in \Sigma$ .

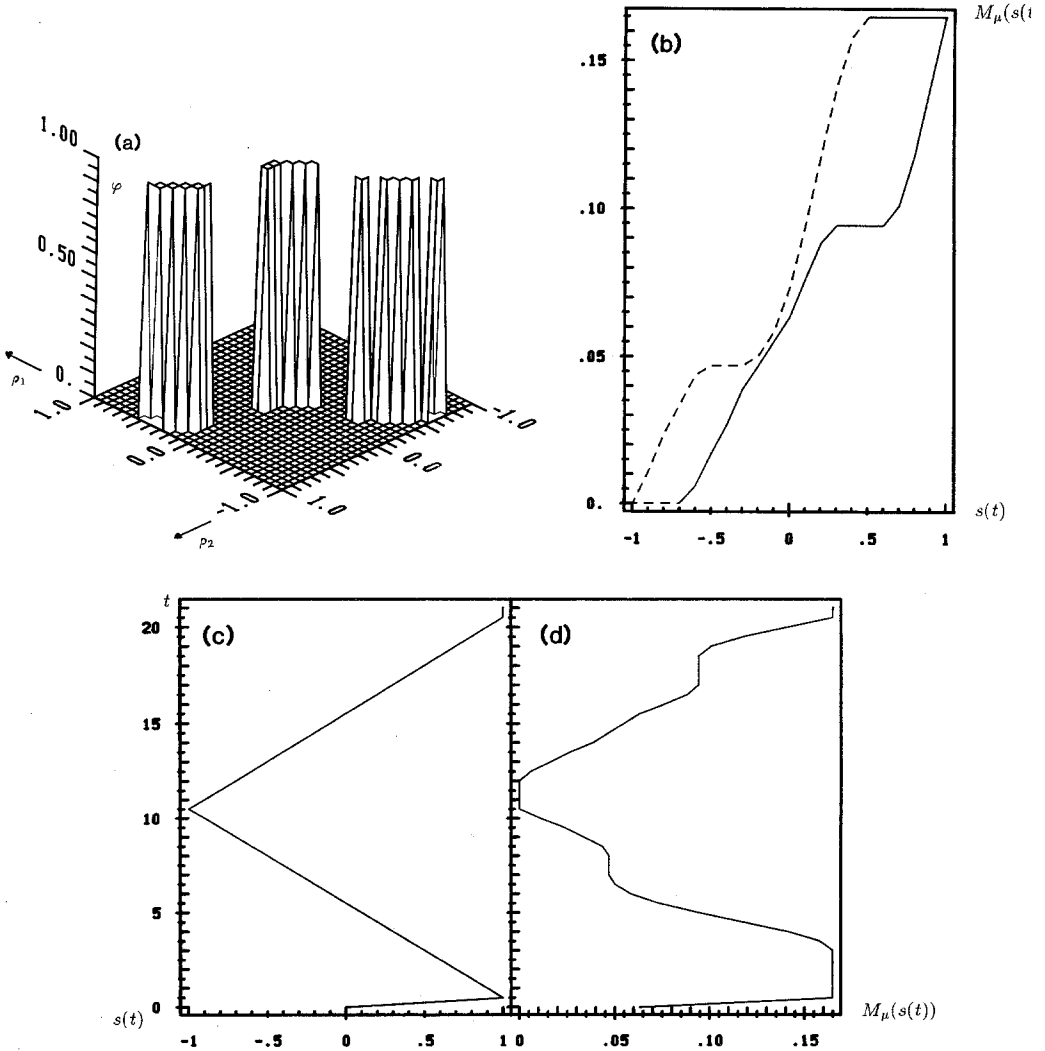


FIG. 7. Example 3.

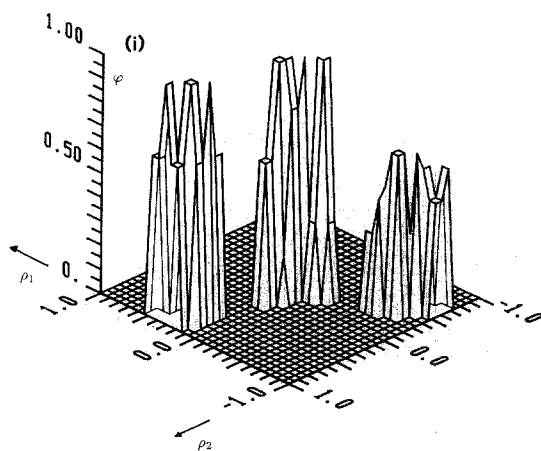
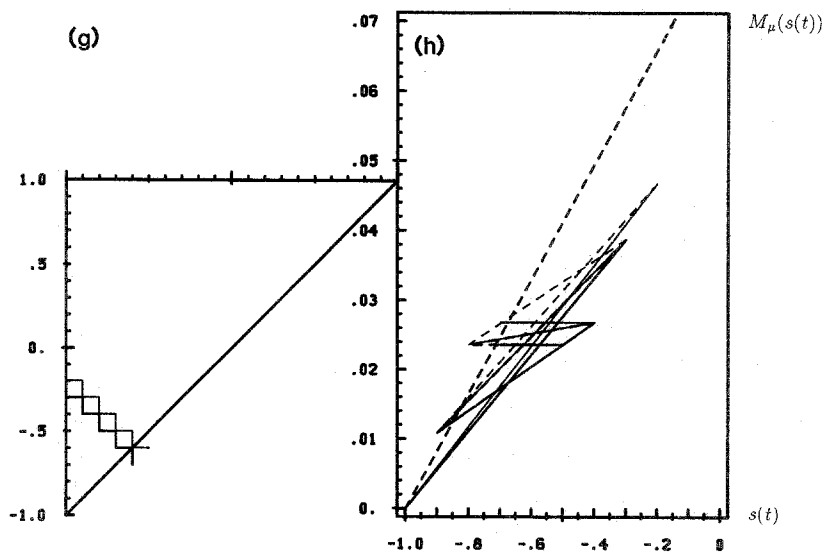
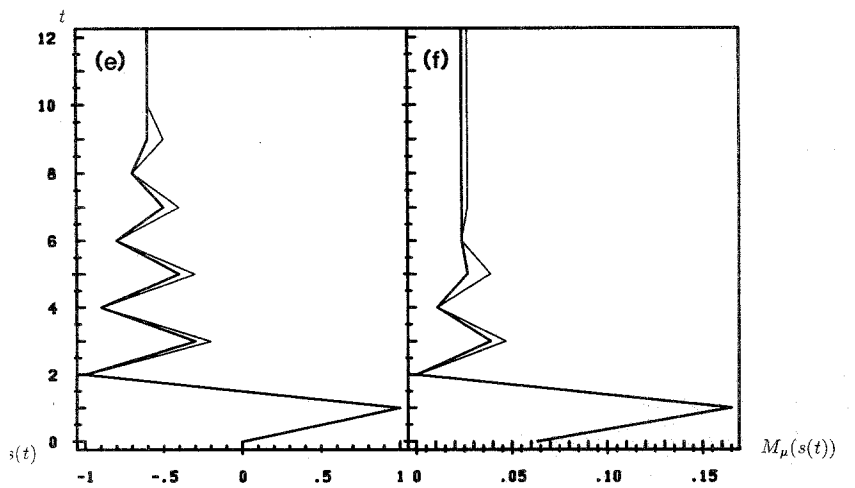


FIG. 7—Continued.

EXAMPLE 2.  $\Sigma L = -1$ ,  $\Sigma R = 1$ ,  $m = 10$ :  $\varphi(\rho_1, \rho_2) := \cos((\pi/2)\rho_1) \cdot \cos((\pi/2)\rho_2)$  for  $\rho \in \Sigma$ .

EXAMPLE 3.  $\Sigma L = -1$ ,  $\Sigma R = 1$ ,  $m = 20$ :  $\varphi(\rho_1, \rho_2) \equiv 1$  for  $\rho \in \Sigma$ .

*Concluding Remarks.* (i) A simpler identification procedure can be used if  $\varphi$  is of the form

$$\varphi(\rho_1, \rho_2) = \varphi_1(\rho_1) \cdot \varphi_2(\rho_2),$$

for all  $(\rho_1, \rho_2) \in \mathcal{P}$ ; indeed, in this case, for any non-decreasing (non-increasing, respectively)  $s \in C^0[0, T]$ , we have

$$\begin{aligned} [M_\mu(s, w^0)]|_0^{t'} &= \int_{s(0)}^{s(t')} \varphi_2(\eta) d\eta \\ \left( [M_\mu(s, w^0)]|_0^{t'} &= \int_{s(0)}^{s(t')} \varphi_1(\eta) d\eta, \text{ respectively} \right). \end{aligned}$$

Hence, taking  $s \in C^1[0, T]$  and  $s' \neq 0$ , one obtains

$$\frac{d}{dt} [M_\mu(s, w^0)](t) = \varphi_i(s(t)) \cdot s'(t) \quad (i = 2 \text{ or } 1, \text{ respectively}).$$

(ii) The Preisach model of hysteresis can possibly be used to identify the composition of an alloy ("Preisach spectrograph"). To explain this, let us consider an alloy of two ferromagnetic materials  $A$ ,  $B$ ; let  $\mu_A$  and  $\mu_B$  be the corresponding measures in the Preisach plane. If  $\alpha$  is the percentage of  $A$  in the alloy, then, in a *first approximation*, the measure corresponding to the alloy is  $\mu = \alpha\mu_A + (1 - \alpha)\mu_B$ . Therefore the identification of  $\mu$  allows to establish the percentage  $\alpha$  of the alloy.

#### REFERENCES

1. M. A. KRASNOSELSKII AND A. V. POKROVSKII, *Systems with Hysteresis* (Nauka, Moscow, 1983). [Russian]
2. A. M. ANDRONIKOU, G. A. BEKEY, AND F. Y. HADAEGH, *J. Dyn. Syst. Meas. Control* **105**, 209 (1983).
3. R. E. BELLMAN AND K.-J. ASTROM, *Math. Biosci.* **7**, 329 (1970).
4. G. BIORCI AND D. PESCEITTI, *Nuovo Cimento* **7**, 829 (1958).
5. G. BIORCI AND D. PESCEITTI, *J. Phys. Radium* **20**, 233 (1959).
6. G. BIORCI AND D. PESCEITTI, *J. Appl. Phys.* **37**, 425 (1966).
7. F. PREISACH, *Z. Phys.* **94**, 277 (1935).
8. A. VISINTIN, *Nonlinear Anal.* **9**, 977 (1984).
9. A. FRIEDMAN AND K.-H. HOFFMANN, preprint, Purdue University, Lafayette, Indiana (unpublished).
10. A. VISINTIN, University of Trento, Italy (in preparation).